

# Phases found at grain boundary of $\text{YBa}_2\text{Cu}_3\text{O}_{7-\delta}$ 50 nm films on $\text{SrTiO}_3$ by enhanced anomalous scattering at O:K, Cu:L<sub>2,3</sub> and Ba:M<sub>4,5</sub> edges

J.V. Acrivos\* SJSU, CA 95192-0101

*Dedicated to Nevill Francis Mott, mentor to condensed matter scholars on 100<sup>th</sup> anniversary of his birth 9/30/1905*

## ABSTRACT

A new phase is detected within 100 $\mu\text{m}$  of 24 DEG ab grain boundary (GB) in  $\text{YBa}_2\text{Cu}_3\text{O}_{7-\delta}$  50 nm films on  $\text{SrTiO}_3$  by enhanced (001) anomalous scattering. Site identification and temperature dependence is interpreted using crystallographic weights to distinguish enhanced scattering from total electron yield and fluorescence spectra. The c-axis,  $c_0$  indicates that only ortho-I phase is present far from GB, both ortho-I and II phases are present near GB. The phase  $c_0$  is constant versus temperature across the transition to superconductivity.

\* [jacrivos@athens.sjsu.edu](mailto:jacrivos@athens.sjsu.edu), TEL 408 924 4972, FAX 408 924 4945

keywords: nano-films grain boundary, scattering, superconductivity PACS# 74.25Gz, .72Bk, .78Bz; 78.70Ck, .90+t

## INTRODUCTION

Synchrotron X-ray absorption spectra (XAS) of layered cuprates,  $\text{YBCO}_{x=6.5 \text{ to } 6.9}$  where superconducting planes are intercalated between ionic and perhaps magnetic layers are compared at the O:K, Cu:L<sub>2,3</sub> and the Ba:M<sub>4,5</sub> edges. The film oxygen composition is obtained from the variation in the c-axis,  $c_0$  that determines the (001) enhanced scattered amplitude.

## EXPERIMENTAL

The samples are 50 nm films, grown epitaxially by sputtering in an oxygen atmosphere onto a  $\text{SrTiO}_3$  crystal with and without a 24 DEG ab grain boundary (GB) at the Complutense University and characterized by synchrotron XRD<sup>1</sup>. Spectra were collected versus photon energy, E at LBNL-ALS 6.3.1 station: by the (001) enhanced scattering ( $I_s/I_0$ ) in the Kortright chamber at different temperatures<sup>2</sup> and distinguished from fluorescence ( $F/I_0$ ) and total electron yield (TEY/ $I_0$ ) in the Nachimuthu chamber where E was calibrated at  $E(\text{CuO}, \text{Cu:L}_3)=931.2\text{eV}$ <sup>3</sup>. A plane polarized beam (10 by 100  $\mu\text{m}$  wide) of intensity  $I_0$ , incident on the  $1\text{cm}^2$  film at position x, at fixed angle  $\theta$  to the film ab plane (fig. 1) makes an angle  $2\theta$  with the detector, as reported in each spectrum (fig. 2-5). The samples are identified by whether the film is deposited on a single or a bi-crystal (SC or BC) qualified by the year fabricated/year measured. The oxygen composition is obtained by the comparison to XRD data<sup>1,5</sup>.

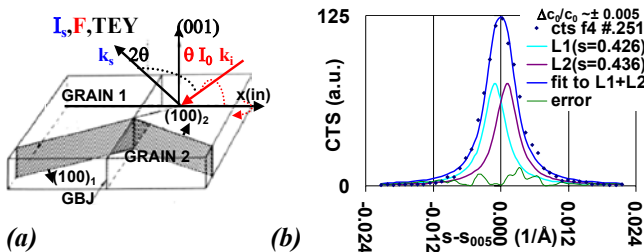


**FIG. 1:** Sample: (a) Measurement geometry determined by the fixed horizontal incident beam  $k_i$ , its position and angle  $\theta$  by the sample displacement and rotation about the x-axis, and  $k_s$  by the detector angle  $2\theta$  to  $k_i$ . (b) BC02/03 (001) XRD versus  $s-s_{005}$   $=2s\sin\theta/\lambda - 5/c_0$ . 100 $\mu\text{m}$  wide beam detected two  $c_0$  at GB [1b].

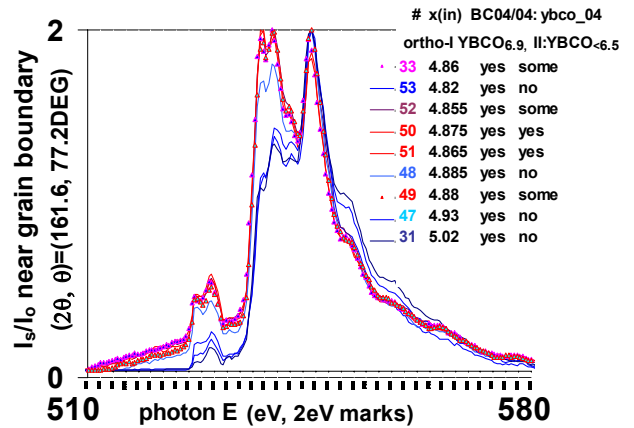


**Figure 2:** Phases detected by  $I_s/I_0$  as incident beam position  $x$  moves across the GB. A new phase is induced within 100 $\mu\text{m}$  of GB ( $\Delta$ ,  $o$ ) detected by enhancement peak at  $\Delta E_{\text{Bragg}} / \langle E_{\text{Bragg}} \rangle \approx -\Delta c_0 / c_0$  from the original  $c_0$  (ortho-I phase)  $\approx 11.6\text{\AA}$  to  $c_0$  (ortho-II phase)  $\approx 11.7\text{\AA}$ .

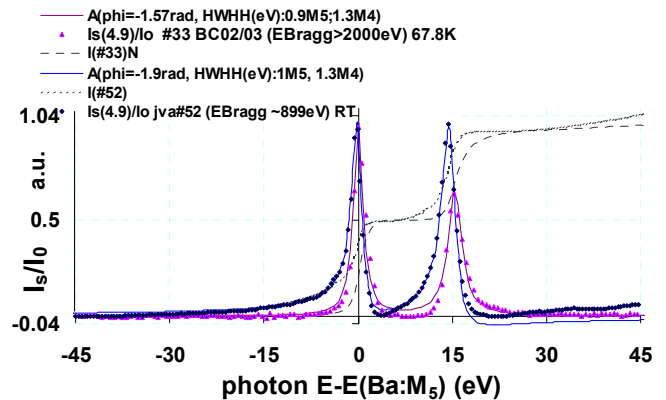


**Figure 3:** Effect of  $E_{\text{Bragg}}$  (2) on  $I_s/I_0$  near the Ba:M<sub>4,5</sub> edges (BC02/03; BC04/04). Lifetime broadening and distortion due to some Ba, commonly occupying Y sites is observed. Broadening is evident in the integrated intensities,  $I$  from 730eV and the fit to  $A$  (4) with different HWHH at the  $M_5$  and  $M_4$  WL, but the integrated intensities remain equal even as the lines narrow.

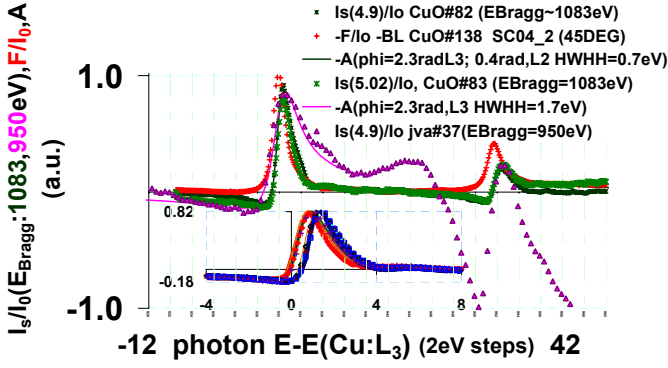


**Figure 4:** Effect of  $E_{\text{Bragg}}$  on  $I_s/I_0$  near the  $\text{Cu:L}_{2,3}$  edges compared to  $F/I_0$  and fitted to relation (4)  $A(L_3)/A(L_2)=3$ ,  $\alpha_{\text{Cu}}$  is constant to 1% in 40eV interval. 100eV broad background at  $E(\text{Cu:L}_3) - E_{\text{Bragg}} \approx 18\text{eV}$  disappears at  $10^2\text{eV}$ . Insert shows reversible 24h cycle of  $I_s/I_0$  versus  $T$  (red  $T > T_c$ , blue  $T < T_c$ ) with  $E_{\text{Bragg}} - E(\text{Cu:L}_3) > 10^3\text{eV}$ .

## DISCUSSION

The YBCO (001) diffraction enhancement is the only one accessible by soft X-rays. The scattering amplitude by atoms  $j$  depends on the incident and scattered photon momenta  $\mathbf{k}_i, \mathbf{k}_s$  (fig. 1a), polarization  $\hat{\mathbf{e}}_i, \hat{\mathbf{e}}_s$  and  $E^{4,6}$ :

$$f_j(\mathbf{k}_i, \mathbf{k}_s, E) = f_j^0(\mathbf{k}_i, \mathbf{k}_s) + \Delta f_j(\mathbf{k}_i, \mathbf{k}_s, \hat{\mathbf{e}}_i, \hat{\mathbf{e}}_s, E). \quad (1)$$

The Thomson amplitude  $f_j^0$  is the matrix element of the square of the vector potential acting on the electron number density. The anomalous amplitude:

$$\Delta f_j(\mathbf{k}_i, \mathbf{k}_s, \hat{\mathbf{e}}_i, \hat{\mathbf{e}}_s, E) = f_j^2 + i f_j^{\prime\prime} \approx \sum_j \sum_{n,l} [\langle \hat{\mathbf{e}}_s, \boldsymbol{\mu}_{ln} | e^{-i\mathbf{k}_s \cdot \mathbf{r}_j} \rangle \langle e^{i\mathbf{k}_i \cdot \mathbf{r}_j} | \boldsymbol{\mu}_{nl}^* \cdot \hat{\mathbf{e}}_i \rangle ] / [E_n - E_l + E + (\Delta_n - i \text{HWHH})] + \text{HC}$$

involves dipole matrix elements  $\boldsymbol{\mu}_{ln}$  between initial and final states  $(n,l)$  with energies  $E_n, E_l$ , that depend on orientation in a layer cuprates<sup>7</sup> (incident  $\boldsymbol{\varepsilon}_{\text{X-ray}}$  unit vector,  $\hat{\mathbf{e}}_i$  is in the film ab plane), state lifetime that determines the half width at half height HWHH, crystallographic site diffraction weights  $\alpha_j = \sum_j e^{i(\mathbf{k}_i - \mathbf{k}_s) \cdot \mathbf{r}_j}$ ,  $\Delta_n =$  Lamb shift,  $f_j^2 =$  dispersion,  $f_j^{\prime\prime} =$  absorption, HC=Hermitean conjugate, and the Bragg relation:

$$E_{\text{Bragg}} = hc/2\sin(\theta)/c_0 + \text{Stenström correction}(\theta) \quad (2)$$

is determined by the magnitude of the  $c$ -axis,  $c_0$ ,  $h =$  Planck constant,  $c =$  velocity of light. Hanzen<sup>5a</sup> has correlated the oxygen composition of  $\text{YBCO}_{x=7-8}$  with  $c_0$  in each phase. Thus at fixed orientation, minute changes:

$$\Delta E_{\text{Bragg}}/E_{\text{Bragg}} \sim -\Delta c_0/c_0. \quad (3)$$

can detect the appearance of new phases as the incident beam scans the film surface with fixed  $\mathbf{k}_i, \mathbf{k}_s$  (fig. 1a). As  $E \Rightarrow E_{\text{Bragg}}$  the edge white line (WL) lifetime broadening increases, due to the detection of enhanced quadrupole transitions and/or enhanced Compton and Rayleigh scattering. As  $E_{\text{Bragg}} - E$  increases, the tail of  $f^0$  becomes a baseline correction (fig. 2-5), but the film may rotate the plane polarized light by an angle  $\phi$ . Then the signal and its Hilbert-Kramers-Kronig transform:

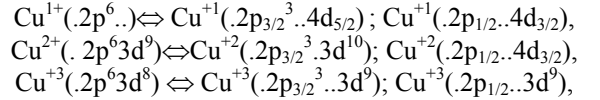
$$\left( \begin{array}{c} I_s / I_0(E) \\ \int_{-\infty}^{\infty} \frac{2 I_s / I_0(E')}{\pi (E' - E)} dE' \end{array} \right) = \left( \begin{array}{cc} \cos(\phi) & -\sin(\phi) \\ \sin(\phi) & \cos(\phi) \end{array} \right) \left( \begin{array}{c} \text{Re} \Delta f \\ \text{Im} \Delta f \end{array} \right)$$

are a mixture of real, R and imaginary, I terms in  $\Delta f$ . The data (fig. 2-5) are analyzed with the purpose to ascertain the properties of films with GB for proper industrial use:

(i) A mixture of real and imaginary components is observed in the WL at the  $\text{Cu:L}_{2,3}$  and  $\text{Ba:M}_{5,4}$  (fig. 3, 4) for BC and SC films where  $\text{TEY}/I_0$  and  $F/I_0$  show a Lorentzian shaped WL with an edge jump weaker than 1% of WL amplitude<sup>7</sup>. Thus if the  $f^0$  tail is linear, the enhanced scattered amplitude minus a base line may be compared to:

$$A_j = I_{sj}/I_0/\alpha_j = [y \cos(\phi) - \sin(\phi)]/[1 + y^2] \quad (4)$$

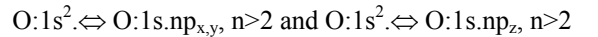
where  $y = (E - E_0)/\text{HWHH}$ ,  $E_0$  is the edge energy and HWHH is the WL half width at half height. The fitted A indicate that the film rotates the plane polarized beam by  $\phi(\text{Cu:L}_3) \approx 3\pi/4 \pm \pi$  at  $E(\text{Cu:L}_3) - E_{\text{Bragg}} = 18$  to  $10^2\text{eV}$ , and  $f^{\prime\prime} \approx I_s/I_0(E_{\text{Bragg}})$  (fig. 4) agrees with theory  $\phi \approx 0^4, 6$ . The observed lifetime broadening<sup>6b</sup> narrows to HWHH=0.7 from 1.7eV when  $E_{\text{Bragg}} - E(\text{Cu:L}_3) = 10^2$  and 18eV, respectively. WL transitions at  $L_{2,3}$  edges (fig. 4) depend on the Cu valence:



the crystal field splitting (different at the  $L_2$  and  $L_3$  edges) and orientation<sup>7-9</sup> making it difficult to assign spectral features to the Cu sites in  $\text{YBCO}_x$ . Site identification is made by the variation in  $\alpha_j(E) = n_j \cos(2\pi z_j E/E_{\text{Bragg}})$  versus different fixed  $E_{\text{Bragg}}$ , when  $n_j$  is the number of equivalent atom  $j$  sites with coordinate  $z_j$  in the unit cell (Table I). When  $E(\text{Cu:L}_2) \approx E_{\text{Bragg}} \approx 950\text{eV}$ ,  $\alpha_{\text{Cu:2}}/\alpha_{\text{Cu:1}} \approx -1.4$  the enhanced shoulders  $\sim 6\text{eV}$  above the main signal, but of opposite sign amplitude may be due to the Cu:1 site contribution. The exact cancellation expected for  $E_{\text{Bragg}} = 1083\text{eV}$ ,  $\alpha_{\text{Cu:1}}/\alpha_{\text{Cu:2}} \approx -1$ , if the second order matrix elements in  $\Delta f_{\text{Cu}}$  for both sites are of the same order of magnitude, is not observed, indicating that Cu:1 and Cu:2 appear at different  $E$ , with a different Cu valence and  $\phi(\text{Cu:2}) \approx 3\pi/4$ .

(ii) Data at the O:K edge indicate that a displacement of the 100 $\mu\text{m}$  wide beam, across the GB detects a new enhancement peak, associated with a higher  $c_0$  phase. The relative amplitude (fig. 2, #50, 51) in the XAFS region centered at 538eV ( $c_0 \approx 11.7\text{\AA}$ ) identifies it with the ortho-II phase ( $\text{YBCO}_{<6.5}$ ) relative to that at 546eV ( $c_0 \approx 11.6\text{\AA}$ ) for the ortho-I phase ( $\text{YBCO}_{6.9}$ ) in agreement with the XRD data<sup>1b</sup>. The width of the GB is comparable to the beam width since full enhancement, at  $E_{\text{Bragg}} \approx 538\text{eV}$  appears only within  $x \approx 4.87 \pm 0.005\text{in}$ , while that at 546eV decreases very little across the GB. Comparison to  $c_0$  data versus O composition<sup>5</sup> indicates that near the GB a  $\sim 5\%$  discontinuous O decrease induces the ortho-II phase which releases the film strain, by creating the  $k_x = -k_y$  periodic lattice distortions (PLD) observed in XRD for the film<sup>1b,c, 8c</sup>.

The information obtained on  $\text{YBCO}_x$  transitions:



when  $\hat{\mathbf{e}}_i$  is in the ab plane is according to relation (1). Comparison of enhancement at  $E_{\text{Bragg}} = 545$  and  $2 \cdot 10^3\text{eV}$  (Table I, fig. 5 #37, 28) identifies the site contributions.  $I_s/I_0$

near 528, 538eV is identified with O:2 by the doubling of  $\alpha(O:2)$  and orientation independent amplitude maximum in  $F/I_0$ , expected in a nearly local octahedral field.  $I_s/I_0$  near 530eV is identified with O:1 by the relative amplitudes  $\alpha(O:2)/\alpha(O:1)=0.8$  and 1.9, and  $I_s/I_0$  near 531eV to 536eV is identified with O:3<sub>A,B</sub> by  $\alpha(O:3_{A,B})$  sign changes:

$$I_s/I_0(\alpha(O:3_{A,B}) \approx -2.7) \leq 0 \text{ while } I_s/I_0(\alpha(O:3_{A,B}) \approx 3.5) > 0.$$

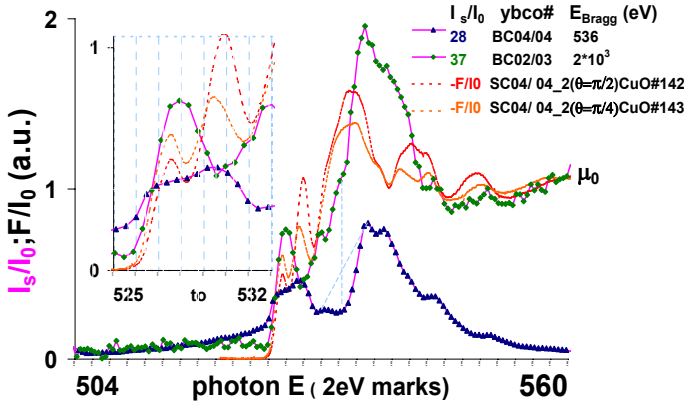
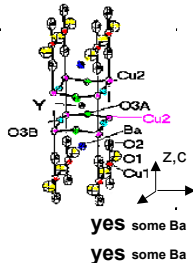


**Figure 5:** O:K edge comparison of  $I_s/I_0(E_{\text{Bragg}} \approx 536$  and  $2 \cdot 10^3 \text{ eV})$  with  $F/I_0$ , normalized to XAFS:  $\mu_0 = 1$ , and  $I_s/I_0$  to constant  $\alpha(O:1)$  at  $\sim 530 \text{ eV}$  identify O:2 and O:3<sub>AB</sub> site contributions by the variation in  $\alpha$  versus  $E_{\text{Bragg}}$  (Table I).

Assignments made by a single diffraction with soft X-rays using the variation of  $\alpha$  versus  $E_{\text{Bragg}}$  are similar to those made by different measurements<sup>8</sup> for de-twinned single crystals YBCO<sub>x</sub>, and may be correlated to the chemical valence: The most negative ionic valence is associated with the lowest energy for site O:2 in the BaO layer, the next higher energy with site O:1 in the CuO chains and the highest valence is assigned to sites O:3<sub>A,B</sub> where molecular orbital calculations show that the CuO<sub>2</sub> layer in YBCO<sub>x</sub> nano-particles is covalent with a Mulliken atomic charge at the O:3<sub>A,B</sub> sites of  $-1.3$  and  $0.8$  at the Cu:2 sites<sup>1c,9</sup>.

**Table I:** Assignment of the YBCO<sub>x</sub> unit cell sites, Hanzen notation<sup>5a</sup> by correlation of  $I_s/I_0$  to crystallographic diffraction weights  $\alpha$  when  $E = E_{\text{Bragg}}$  and  $E \neq E_{\text{Bragg}}$  (fig. 2- 5).

YBCO <sub>x</sub>	D <sub>2h</sub> <sup>17</sup>	Site:	O:1	O:2	O:3A,B	Cu:1	Cu:2	Ba	Y
(001) enhancement	z:		0	$\pm .18$	$\pm .378$	0	$\pm .358$	$\pm .18$	$\pm .5$
	$\alpha(E_{\pm})$ :		1	0.8	-2.9	1	-1.4	0.8	-1
$I_s/I_0$ Peak		$\alpha(E_{\mp})$ :	1	1.9	3.4	1	-1	1.9	0.6
E (eV)	Sign	$I_s/I_0$	Site Contribution to Signal						
528	+	+	yes						
530	+		yes						
531-535	-				yes				
531-535	+	+			yes				
538	+		maybe	yes					
545	+				yes				
779	+	+							
793	+	+							
932	$\pm$	$\pm$							yes
950	$-\pm$	$\pm$							yes
936	$-\pm$								yes
954	$-\pm$								yes



Temperature dependence measurements indicate that  $c_0$  is unchanged across  $T_c$  by the constant enhancement peak observed at  $E_{\text{Bragg}} \approx 546 \text{ eV}$  in the ortho-I phase.  $\phi(\text{Cu}:2:L_{3,2}) \approx 3\pi/4$  in (4) is constant across  $T_c$ , but a reversible 0.5eV edge shift below  $T_c$ , observed at the Cu:2:L<sub>3,2</sub> edges in a 24 h, T cycle (fig. 4 insert) is assigned to an increased Cu:2 site valence below  $T_c$ .

(iii) In the ideal YBCO<sub>x</sub>, Ba occupies a unique site but in real crystals it also occupies Y sites. As  $E_{\text{Bragg}} - E(\text{Ba}:M_5) = -38$  to  $2 \cdot 10^3 \text{ eV}$  lifetime broadening is observed when  $\alpha_{\text{Ba}}/\alpha_Y \approx -0.8$  but the WL narrow for  $\alpha_{\text{Ba}}/\alpha_Y \approx 3$  (Table I, fig. 3 #52 and #33). Amplitudes for WL transitions:

$\text{Ba}^{2+}(.3d^{10}) \leftrightarrow \text{Ba}^{+2}(.3d_{5/2}^5 .4f_{7/2})$ ;  $\text{Ba}^{+2}(.3d_{3/2}^3 .4f_{5/2})$ , are proportional to the initial state multiplicities,  $A_{M5}/A_{M4} = 1.5$  only for  $E_{\text{Bragg}} - E > 2 \cdot 10^3 \text{ eV}$ . The TEY/ $I_0$  for BC04/04 are orientation dependent<sup>7c,9</sup>.

## CONCLUSION

The fabricated nano-film YBCO<sub>x</sub> (001) anomalous enhanced scattering analysis, sensitive to phase and O composition characterizes the GB for device applications and theoretical interpretation of transport data.

## ACKNOWLEDGEMENTS

Work was supported by the NSF and Dreyfus Foundations at SJSU, DOE at LBNL-ALS and scholars<sup>1-9</sup>.

## REFERENCES

- [1](a) M. A. Navacerrada, M. L. Lucía and F. Sánchez-Quesada, *Europhys. Lett* **54**, 387 (2001); (b) M.A. Navacerrada and J.V. Acrivos, *NanoTech2003*, **1**, 751 (2003); (c) H.S. Sahibudeen, J.V. Acrivos and M.A. Navacerrada, *Nanotech 2005*, **2**, 573 (2005)
- [2] J.B. Kortright et al., *J. Magn. Magn. Materials*, **207**, 7 (1999)
- [3] P. Nachimuthu et al., *Chem. Mater.* **15**, 3939 (2003)
- [4] (a) R.W. James, "The optical principles of X-rays", Ox Bow Press, Woodbridge, Conn. 1962; (b) L.K. Templeton and D.H. Templeton, *Acta Cryst.* **A47**, 414 (1991)
- [5](a) R.M. Hazen et al., "Physical Properties of High Temperature Superconductors, II" p. 121, D.M. Ginsberg, ed, World Scientific, Singapore (1990); (b) N.H. Andersen, *Physica C*, **317-318**, 259 (1999)
- [6] (a) L.B. Sorensen et al., "Diffraction anomalous fine structure" North Holland, G. Materlik et al., ed (1994) p.389; (b) Hämäläinen, et al., *ibid* p. 48; (c) J.C. Woicik et al., *Phys. Rev.B* **58**, R4215 (1998)
- [7](a) A. Bianconi et al, *Phys. Rev.B* **38**, 7196 (1988); (b) F.M.F. de Groot et al., *ibid. B* **42**, 5459 (1990); (c) J.V. Acrivos et al., arKiv, cond-mat/0504369
- [8](a) M. Merz, et al., *Phys. Rev. Lett.* **80**, 5192 (1998); (b) J.H. Guo et al., *Phys. Rev. B* **61**, 9140 (2000); (c) E. Bascones et al., *ibid*, **71**, 012505 (2005)
- [9](a) J.V. Acrivos, *Solid State Sciences*, **2**, 807 (2000); (b) J.V. Acrivos et al., *Microchemical Journal*, **71**, 117 (2002); *ibid*, **81**, 98 (2005)